PCCP

PAPER

View Article Online
View Journal | View Issue

Check for updates

Cite this: *Phys. Chem. Chem. Phys.*, 2025, **27**, 15350

In vitro analysis of β-carotene supplementation: insights from Raman spectroscopy on brain, lung, and breast cancer cells†

Karolina Jarczewska, Monika Kopeć and Jakub Maciej Surmacki *

Received 3rd April 2025,
Accepted 1st July 2025

DOI: 10.1039/d5cp01289a

rsc.li/pccp

β-carotene, a carotenoid abundant in fruits and vegetables such as carrots and tomatoes, plays a significant role in human health and its potential in cancer prevention is widely discussed. However, its precise impact on tumour cell metabolism remains unclear. Utilizing Raman spectroscopy, a technique adept at analysing complex biological systems, we investigated the effects of β-carotene on lung (A549), breast (MCF7), and brain (CRL-1718) cancer cells. We have found that the supplementation with 1 and 10 μM β-carotene altered lipid metabolism differently across cancers: increased lipid production and cytochrome *c* redox changes in lung cancer, and inhibited growth with reduced lipid and protein levels in breast and brain cancers. Those changes are observed based on a detailed analysis of recorded Raman spectra. We have chosen Raman bands at 1003, 1254, 1310, 1444, 1654, 2848–2964 cm^{-1} as biomarkers. These findings suggest that β-carotene influences cancer cell metabolism in unique ways, supporting its potential role in cancer treatment strategies.

Published on 04 July 2025. Downloaded on 5/25/2026 7:46:48 AM.

Introduction

According to the World Health Organisation's 2024 statistics, lung cancer is the most deadly cancer in men and women, and breast cancer is the second most deadly cancer in women.[1] Brain tumours are dangerous mainly because of the pressure on other parts of the brain, which can affect a person's functioning. Although brain tumours are not common, they are among the top ten most deadly cancers.[1] Carcinogenesis affects mostly cellular energy metabolism, to proliferate faster, cancer cells redirect metabolism to glycolysis regardless of the presence of oxygen.[2,3]

Lung cancer has been identified as the leading cause of cancer deaths among both sexes in the United States (population 333.3 million in 2022) and among men worldwide.[4,5] The most common symptoms of lung cancer are prolonged cough, shortness of breath, wheezing, hoarseness, chest and arm pain, constant fatigue, and swelling of the face and neck. A key factor in the development of lung cancer is smoking. Lung cancer usually arises from exposure to carcinogens in tobacco smoke, not only traditional cigarettes, but also more popular electric cigarettes nowadays. Other factors include polluted air, exposure to asbestos or radon and genetic background.[6] It has been reported that c-*myc*, mutated K-*ras* and overexpressed EGFR, cyclin D1 and BCL2 are oncogenes that contribute to the pathogenesis of lung cancer.[7,8] There are two main types of lung cancer: small cell carcinoma and non-small cell carcinoma (adenocarcinoma, squamous cell carcinoma and large cell carcinoma).[9,10] Diagnosis of lung cancer includes X-ray, CT scan, positron emission tomography, MRI, or chest ultrasound.[11–13] Once the tumour is detected and localised, the main investigation is a biopsy. Usually, the tumour is surgically removed, and chemotherapy or radiotherapy is implemented. New treatments such as targeted molecular treatment or immunotherapy are currently being developed.[10]

Breast cancer is one of the most common cancers in women. It has been reported that malignant transformation is connected to the dysregulation of fatty acid metabolism in breast cancer.[14] The change in metabolism occurs also in mitochondria.[15] Breast cancer arises mainly from breast cells and, if malignant, can metastasise to lymph nodes or other organs such as the lungs.[16] Most breast cancer cases originate in the ducts and far fewer in the lobules. It is a dangerous disease because it usually does not produce any symptoms for a long time. When it is detected, it has often already metastasised. Obesity, physical inactivity, alcohol abuse and ionising radiation are common factors in the development of breast cancer.[17,18] Some breast cancers have a genetic basis - if there is a family history, subsequent generations are at higher risk. There are many programmes to improve breast cancer

Lodz University of Technology, Faculty of Chemistry, Institute of Applied Radiation Chemistry, Laboratory of Laser Molecular Spectroscopy, Wroblewskiego 15, 93-590 Lodz, Poland. E-mail: jakub.surmacki@p.lodz.pl; Tel: +48426313188

† Electronic supplementary information (ESI) available. See DOI: https://doi.org/10.1039/d5cp01289a

This journal is © the Owner Societies 2025

Published on 04 July 2025. Downloaded on 5/25/2026 7:46:48 AM.

diagnosis, such as free mammography for women over sixty, but this still does not improve the diagnosis enough.[19]

The brain is the centre of the human nervous system. It is the most complex organ in the entire body. Brain cells are neurons that are capable of processing and conducting information in the form of an electrical signal.[20,21] Neurons are present in the brain and throughout the body, where they are connected by synapses.[22] The role of the brain is to control all processes in the body.

It is well known that diet is a key factor affecting health. Various diseases result from a poor diet, such as diabetes,[23–27] obesity,[28–31] cardiovascular disease[32] or osteoporosis.[33–36] It has been reported that some cancers are diet-dependent.[37–39] Instead, a proper and well-balanced diet may be important in cancer prevention. During cancer treatment, such as chemotherapy, diet plays a key role in recovery. The amount of nutrients required to recover from cancer is much higher than in a standard diet, so special nutrition should be implemented. A diet rich in fruit and vegetables has been proven to be the key to preventing disease or recovering faster.

β-carotene is the most common carotenoid, present in various diets, which can be converted into vitamin A (retinol). Sources of β-carotene include plants such as carrots, spinach, lettuce, broccoli or pumpkin, fruits such as melons or oranges and egg yolks.[40–42] Fig. 1 shows the structural formula of β-carotene and its typical sources.

Its functions in the human body are to prevent from reactive oxygen species (ROS), participate in the formation of melanin, collagen and facilitate the binding of minerals, thus improving bone structure. β-carotene stimulates the immune system and prevents inflammation.[43] Its ability to prevent from ROS is valuable in cancer prevention. Furthermore, being a precursor to vitamin A, which is responsible for cell differentiation, also indicates that β-carotene may inhibit cancer development.[44–46]

β-carotene in the human body is cleaved at the 15,15′ double bond by β-carotene-15,15′-oxygenase and generates two molecules of retinaldehyde. It can be oxidised to retinoic acid by the aldehyde dehydrogenase family of enzymes. Further oxidation of retinoic acid by the cytochrome P450 (CYP) 26 family converts retinoic acid to 4-oxo-retinoic acid, which is more polar. Other alcohol dehydrogenases and retinol dehydrogenases can reduce retinaldehyde to retinol. This can be esterified to retinyl esters. Apo-carotenes can be generated from β-carotene when cleavage occurs at the 9′,10′ double bond.[42,47,48] In many research or industrial applications, there is a need to quantify β-carotene or its metabolites. To date, the most popular methods have been high-performance liquid chromatography (HPLC), gas chromatography (GS) and mass spectrometry (MS).[49] However, these methods require extraction of the sample and thus its destruction. When there is a need to analyse β-carotene in cellular metabolism, information on the location of metabolites is crucial. To address this, we implemented Raman spectroscopy (RS) and imaging. These techniques have proven to be a valuable tool for the analysis of carotenoids and retinoids.[50–54]

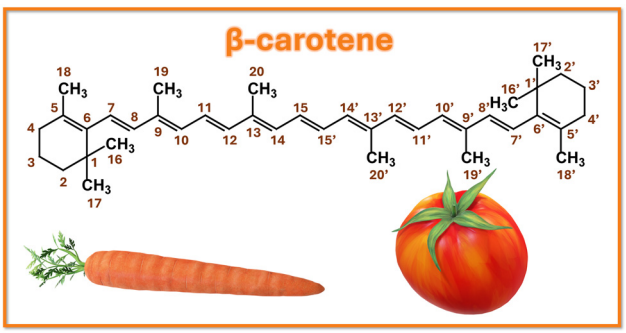

Fig. 1 The structural formula and main sources of β-carotene.

A phenomenon of the Raman effect is based on the interaction between light and a molecule. When the energy of an incident photon is different than the energy of the molecule, the light is scattered inelastically. Around 1 in 10^{10} of the light is scattered inelastically at a different wavelength than the incident light.[55,56] RS analyses the scattered light and enables the analysis of solid and liquid samples. In biological applications, RS has proven to be a valuable tool because it is non-destructive, label-free and requires minimal sample preparation.[57,58]

It is well known that β-carotene plays a significant role in human health. Although its potential in cancer prevention is widely discussed, its precise impact on tumour cell metabolism remains unclear. To answer the question of how to improve cancer prevention in human globally, we proposed a study on the effects of β-carotene on brain, breast and lung cancer cells analysed by Raman spectroscopy and imaging.

Materials and methods

Chemicals

The β-carotene (no. C9750) was purchased from Merck Life Science.

Cell culture and preparation for microscopy

Cancer cell lines, brain astrocytoma CRL-1718 (no. CCF-STTG1), breast adenocarcinoma MCF7 (no. HTB-22) and lung A549 (CCL-185) were purchased from ATCC. We selected cancerous cell lines based on their representation of mildly aggressive tumours. CRL-1718 was cultured on RPMI-1640 medium (no. 30-2001, ATCC). MCF7 was cultured on Eagle's Minimum Essential Medium (EMEM, no. 30-2003, ATCC). A549 was cultured on Kaighn's Modification of Ham's F-12K Medium (no. 30-2004, ATCC). To each medium Fetal Bovine Serum (FBS, no. 30-2020, ATCC) was added to a final concentration of 10%. Media were renewed twice a week, and the subculturing was done once a week. Cells were cultured in T75 sterile, flat-bottom flasks (no. 90076, Techno Plastic Products). Cells were maintained in a humidified atmosphere incubator at 37 °C with 5% of CO_2.

Preparation for microscopy was done 24 hours before supplementation. Cells were seeded on CaF_2 windows (no. CAFP25-1R Crystran Ltd, Poole, UK) in Petri dish (no. 150460, Nunc). 10

Published on 04 July 2025. Downloaded on 5/25/2026 7:46:48 AM.

mM β-carotene solution was prepared by dissolving the proper amount of β-carotene powder in dimethyl sulfoxide (DMSO, no. 4-X, ATCC). On the day of supplementation, CRL-1718, MCF7 and A549 cell's media were changed for the solution of β-carotene in RPMI-160, EMEM and F-12K media, respectively. 1 and 10 μM concentrations were investigated. These concentrations were chosen to present two extremes - low, close to the actual conditions found in cells after dietary supplementation, and high, likely to have a therapeutic effect.

After 24 or 48 hours, media were removed, and cells were rinsed with phosphate-buffered saline (PBS, no. 10010023 Gibco) and fixed in 4% formalin (neutrally buffered). Cells in PBS were measured by Raman imaging.

Raman spectroscopy and imaging

All Raman spectra and images presented in this manuscript were obtained using a WITec Alpha 300 RSA+ confocal microscope (Ulm, Germany). This microscope was coupled to an enhanced mode CCD camera (EMCCD, Andor Newton DU970N-UVB-353). Experiments were carried out using a laser with an excitation wavelength of 532 nm and a laser power of 10 mW and a 40× objective with an aqueous solution cap (Zeiss). The integration time was 0.5 seconds for the range from 400 to 1800 cm^{-1} and 0.3 seconds for the range from 2700 to 3100 cm^{-1}. Each Raman spectrum and image were pre-processed for smoothing (Savitzky–Golay method, order 4, derivative 0), cosmic ray removal (filter size 2, dynamic factor 10) and background subtraction using WITec Project Plus software. Raman images were recorded with 1 × 1 μm spatial resolution. Total amount of analysed samples was 15 : 3 control samples and 4 supplemented for each cell line. From each sample, four cells were measured, which gave the total amount of measured cells: 60. For A549 cell line, we analysed 14 128 spectra for control cells and 24 864 spectra for supplemented cells. For MCF7 cell line, we analysed 5191 spectra for control cells and 21 424 spectra for supplemented cells. For CRL-1718 cell line, we analysed 9580 spectra for control cells and 32 416 spectra for supplemented cells. The average size of one Raman image was 40 × 45 μm, which gives 1800 spectra for one cell and one spectral region. Raman maps were analysed using a Cluster Analysis method.[3,59] This approach enables segmentation of spectral data into distinct groups sharing common vibrational signatures. Cluster analysis was conducted using WITec Project Plus software, with the number of clusters set to six. Each Raman map was analysed independently, preserving spatial resolution and mitigating potential misclassification arising from heterogeneity in cell morphology, size, and micro-environmental conditions. There were six clusters corresponding to cell organelles: nucleus (red), mitochondria (magenta), lipid droplets/endoplasmic reticulum (blue), cytoplasm (green), cell membrane (light grey) and the extracellular region (dark grey). Mean and standard deviation calculations were performed in Origin Pro. Statistical analysis, one-way ANOVA with Tukey's tests was performed to denote statistical differences. If the *p*-value was less than or equal to 0.05, we marked the difference as significant with an asterisk (*). PLS-DA, a chemometric analysis was performed using MATLAB. Prior to Partial Least Squares Discriminant Analysis (PLS-DA), spectral data were vector normalized using the ''Divide by Norm'' method in Origin Pro to compensate for possible variations in overall signal intensity. For the PLS-DA model, dummy variables were assigned according to the experimental groups corresponding to controls and supplemented samples (as presented on Fig. 9). The classification parameter was based on these categorical group assignments, allowing the model to discriminate between the biochemical profiles associated with each condition. The optimal number of latent variables was determined by cross-validation to avoid overfitting and ensure robustness of the model. Six discrete classes were defined for classification, with mean centring applied to enhance data variance structure. The PLS-DA model was constructed using five latent variables, optimized to capture the maximum covariance between spectral features and class membership.

Results and discussion

The aim of our study was to investigate how β-carotene affects lung, breast and brain cancer cells using Raman imaging. We analysed cells without supplementation (control) as reference, and cells supplemented with 1 and 10 μM β-carotene.

We started our considerations with an analysis of the control cells. Fig. 2 shows typical Raman images of control cells from cell lines A549, MCF7 and CRL-1718.

Fig. 2 presents Raman imaging of control, non-supplemented cells. Cluster analysis enabled the identification of five distinct cellular domains, corresponding to the nucleus (red), mitochondria (magenta), lipid droplets/endoplasmic reticulum (blue), cytoplasm (green) and cell membrane (grey). Each domain exhibited characteristic vibrational signatures. Lipid-rich regions demonstrated prominent Raman bands at 1254, 1444, 1660 cm^{-1} and 2848 cm^{-1}. The nucleus and mitochondria were distinguished by well-defined bands at approximately 785, 1092 cm^{-1} (nucleic acids/DNA) and 750, 1126, 1310, 1583 cm^{-1} (mitochondrial cytochrome *c*), respectively. In contrast, cytoplasm and cell membrane domains displayed generally lower intensities across most Raman bands analysed. However, protein-related amide bands (Amide I and III regions, ∼1654 cm^{-1} and ∼1337 cm^{-1} respectively) are observed throughout the cytoplasm and mitochondria, reflecting the high protein content in these organelles.

Now let us focus on the analysis of supplemented cells. Fig. 3 shows typical Raman images and spectra of β-carotene-supplemented A549, MCF7 and CRL-1718 cells.

Based on the results presented in Fig. 2 and 3, we have demonstrated that Raman spectroscopy and Raman imaging are a suitable tool for the analysis of the structure of cellular organization. Fig. 2 and 3 provide information on the distribution of chemical components in the cells. The Raman bands mode assignments are presented in Table 1.

The prominent Raman bands are at 750, 1003, 1092, 1126, 1254, 1310, 1337, 1444, 1583, 1654, 2848, 2870, 2880, 2900, 2926, 2930 and 2964 cm^{-1}. Moving on to the analysis of

 This journal is © the Owner Societies 2025

Published on 04 July 2025. Downloaded on 5/25/2026 7:46:48 AM.

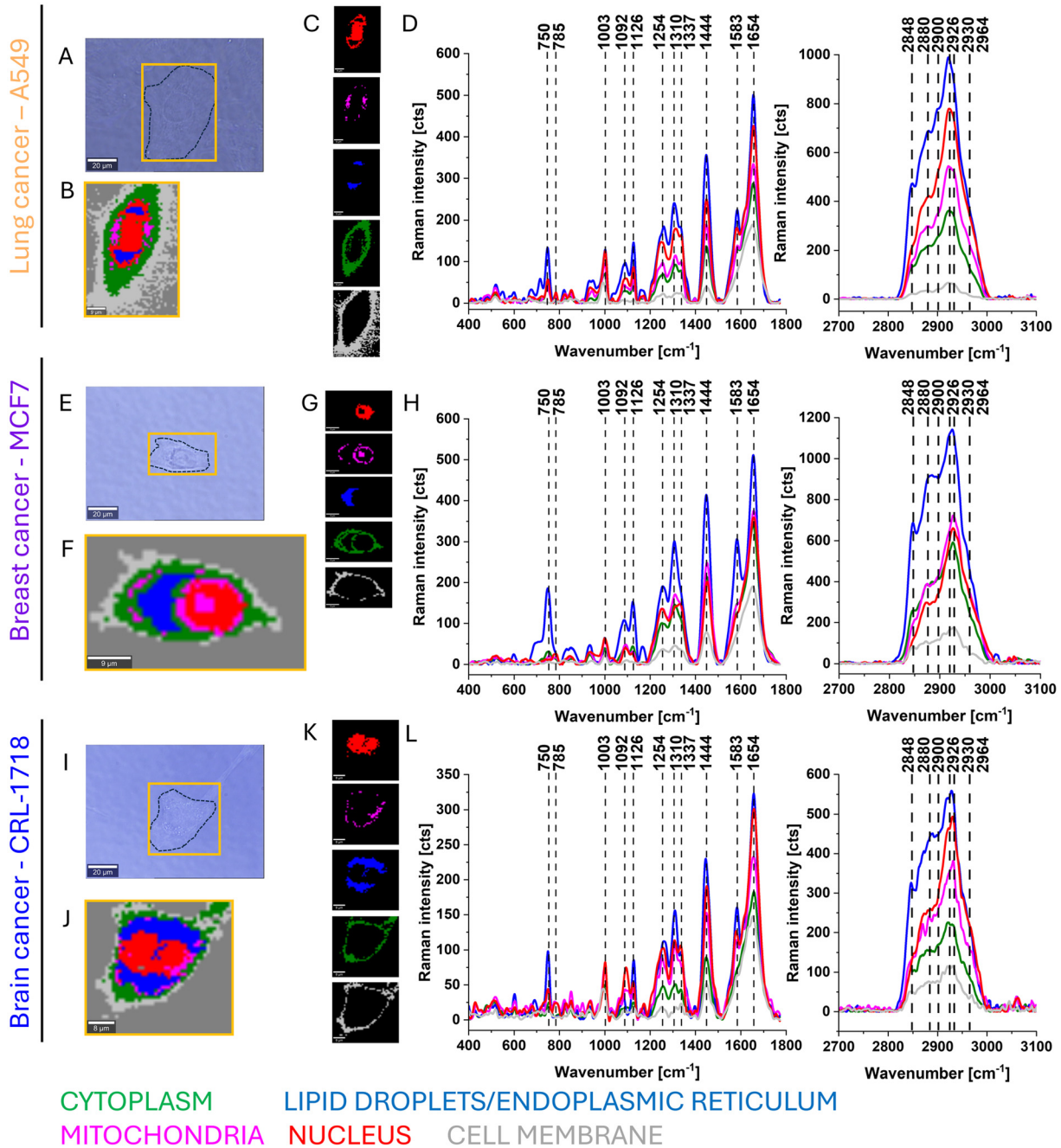

Fig. 2 Typical Raman images of lung cancer (A549), adenocarcinoma (MCF7) and astrocytoma (CRL-1718) cells (controls). The microscope images of cells (A, E and I) with Raman images (B, F and J), Raman images of cell organelles (C, G and K) and representative Raman spectra of cell organelles (D, H and L): nucleus (red), mitochondria (magenta), lipid droplets/endoplasmic reticulum (blue), cytoplasm (green), cell membrane (grey). Resolution of Raman images 1 µm, integration time 0.5 second for range from 400 to 1800 cm^{-1} and 0.3 second for range from 2700 to 3100 cm^{-1}, 10 mW at 532 nm. The colours on the spectra correspond to the Raman images.

individual cell organelles, we will focus on lipid droplets. Fig. 4 shows the average Raman spectra from lipid droplets/endoplasmic reticulum. Each graph shows spectra from control cells and cells supplemented with 1 and 10 µM β-carotene after 24 and 48 hours of incubation with the compound.

Fig. 4 shows the average Raman spectra in two spectral ranges: from 400 to 1800 cm^{-1} and from 2700 to 3100 cm^{-1}. It can be seen that in lung cells the highest intensity of most Raman bands is seen for 10 µM β-carotene after 48 hours. In breast cancer cells, the highest intensity can be observed for control cells. Brain cancer cells showed the highest intensity of most Raman bands for 10 µM β-carotene after 24 hours. Except for the band at 1583 cm^{-1}, where the highest intensity was for 10 µM β-carotene for 48 hours. This indicates that β-carotene induces changes in these organelles, and these changes are different for each organ. In the lung, the highest concentration

Published on 04 July 2025. Downloaded on 5/25/2026 7:46:48 AM.

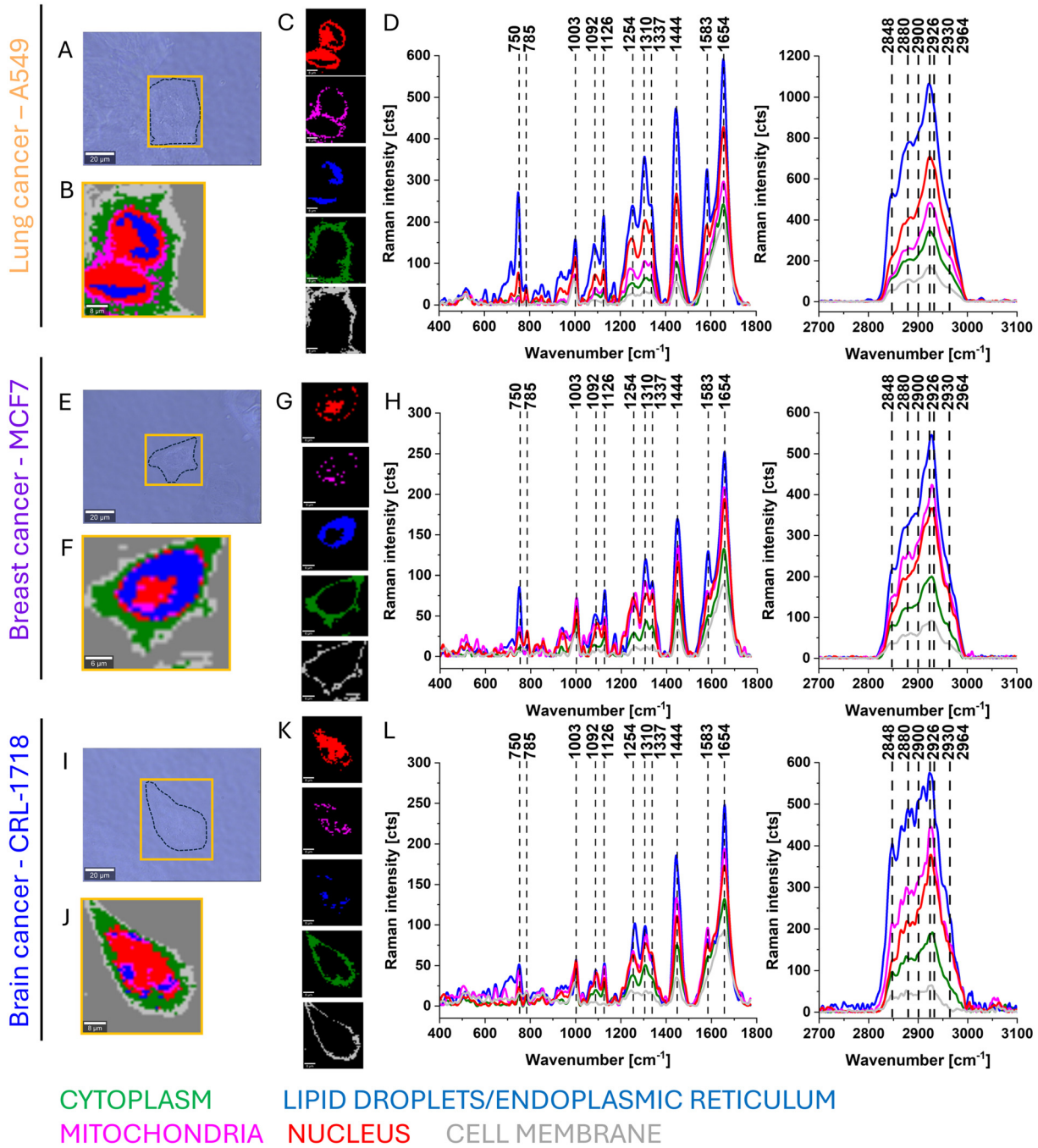

Fig. 3 Typical Raman images of supplemented with β-carotene lung cancer (A549), adenocarcinoma (MCF7) and astrocytoma (CRL-1718) cells. The microscope images of cells (A, E and I) with Raman images (B, F and J), Raman images of cell organelles (C, G and K) and representative Raman spectra of cell organelles (D, H and L): nucleus (red), mitochondria (magenta), lipid droplets/endoplasmic reticulum (blue), cytoplasm (green), cell membrane (grey). Resolution of Raman images 1 µm, integration time 0.5 second for range from 400 to 1800 cm^{-1} and 0.3 second for range from 2700 to 3100 cm^{-1}, 10 mW at 532 nm. The colours on the spectra correspond to the Raman images.

of β-carotene for the longest time results in more lipids (1254, 1444, 1654 cm^{-1}) and proteins (1003, 1654 cm^{-1}) in the lipid droplets/endoplasmic reticulum. In breast cancer, β-carotene supplementation reduced the intensity of most bands and thus the amount of lipids and proteins in lipid droplets/endoplasmic reticulum. In brain cancer cells, the intensities were higher after β-carotene supplementation and therefore the amount of lipids and proteins in this organelle was higher. It has been shown that, regardless of the mechanism of action, excess carotenoids are stored in adipose tissue.[41,44–46] Additionally, we prepared analogous analysis for nucleus (Fig. S1, ESI†) and mitochondria (Fig. S2, ESI†).

Numerous studies have explored carotenoids and their impact on human health.[41,44–46,82] It has been showed that

 This journal is © the Owner Societies 2025

Published on 04 July 2025. Downloaded on 5/25/2026 7:46:48 AM.

Table 1 Raman vibrational mode assignments for the analysed bands in regions 400–1800 and 2700–3100 cm^{-1}

Raman band wavenumber [cm^{-1}]	Raman vibrational mode assignment[55,60–81]
750	Tryptophan (Proteins), cytochrome *c*
785	DNA
1003	Phenylalanine (Proteins)
1092	O–P–O backbone stretching in DNA, symmetric phosphate stretching vibrations, phosphodioxy
1126	C–N stretching in proteins, cytochrome *c*, disaccharides
1254	PO_2^- asymmetric stretching in lipids, C–N in plane stretching, formalin contamination
1310	Guanine–ring breathing mode in DNA, cytochrome *c*, mixed fatty acid chains
1337	Amide III and CH_2 wagging vibrations in DNA, C–H deformation in protein, tryptophan, nucleic acid, cytochrome *c*
1444	Cholesterol, lipids and fatty acids, CH_2 and CH_3 deformation vibrations in lipids, mixed amide I protein
1583	C═C bending mode of phenylalanine, cytochrome *c*
1654–1660	C═C stretching in lipids and proteins, amide I protein
2848	Symmetric stretching of CH_2 of lipids, triglycerides, phospholipids
2870	Symmetric stretching of CH_3 of lipids, CH_2 asymmetric stretch of lipids and proteins
2880	Symmetric stretching of CH_2 and CH_3, and asymmetric stretching of CH of lipids and proteins
2900	CH stretch of lipids and proteins
2926	CH_3 stretching vibrations, CH stretch of lipids and proteins
2930	Symmetric and asymmetric stretching of CH_3 in proteins
2964	Asymmetric stretching of CH_3

carotenoids exert a variety of biological effects, which may be driven by different mechanisms.[82,83] Fig. 5 shows the mechanisms of action of β-carotene. These mechanisms include direct antioxidant actions, redox-sensitive cell signalling, vitamin A signalling pathways, and others.[41,44–46,82]

Carotenoids possess anticancer properties and can prevent the development of various types of cancer, such as bladder, breast, leukaemia, lung, and prostate cancers. The underlying mechanisms of this anticancer activity may vary depending on the specific carotenoid being analysed. These mechanisms include induction of apoptosis and the inhibition of cell proliferation. It should be mentioned that β-carotene is a precursor of vitamin A (retinoid acid) and plays a key role in the differentiation and proliferation of lung epithelial cells. The deficiency or excess of vitamin A can lead to squamous metaplasia of the bronchial epithelium, confirming the critical role of β-carotene in the proper growth and function of lung cells. The metabolic mechanism driving this process is the RAR/RXR-dependent repression of AP1 activity, where AP1 is a transcriptional regulator that responds to external signals, and its activation promotes cell proliferation through the expression of cyclin D1. Squamous metaplasia, a precancerous lesion of the airway epithelium, is induced by the expression of keratins and other proteins.[84] β-carotene in lung cells may undergo oxidation and cleavage to form oxidative metabolites. These metabolites can decrease retinoic acid levels and impair retinoid signalling by down-regulating RAR expression and up-regulating AP1 (activator protein 1). When present in excess, β-carotene may have procarcinogenic effects.[85] In reported study[86] of breast cancer cells, β-carotene has been shown to be an inhibitor of cell proliferation, where stopped the cell cycle progression of MDA-MB-231 cells at the G1 phase. Authors suggested that the antiproliferative effects of β-carotene involve the c-*Jun* N-terminal kinase (JNK) pathway. What is interesting, β-carotene did not affected healthy, control cells viability in this study.[86] β-carotene supplementation reduced the viability of both MCF7 and MDA-MB-231 cells, and decreased the number of cells in the G_2/M and G_0/G_1 phases, respectively.[87] It has also been demonstrated that oxidation products of β-carotene (*e.g.* retinol and retinoic acid) exert effects on breast cancer cells derived from the MCF7 cell line, inhibiting their proliferation.[88]

In breast cancer cells, carotenoids have been shown to downregulate the PI3K/Akt/mTOR signalling pathway and inhibit the RAS/RAF/MEK/ERK1/2 signalling cascade, thereby inhibiting cell proliferation. Carotenoids also block the phosphorylation of IKK protein, preventing the degradation of Iκ-B. Furthermore, carotenoids inhibit the activity of prosurvival proteins (such as Bcl-2 and Bcl-xL) and promote the expression of pro-apoptotic proteins (Bax, Bak, p53), thereby enhancing caspase activity and inducing cell death.[82] It has been suggested that β-carotene regulates the expression of oxidative stress-sensitive genes through the inhibition of Akt and ERK1/2 signalling. β-carotene suppresses the expression of Bcl-2 and NF-κB, thereby activating the caspase 3 family and triggering apoptosis. The influence of β-carotene on brain cancer is thought to be related to its antioxidant properties. Reactive oxygen species (ROS) activate transcription factors such as nuclear factor erythroid 2-related factor 2 (Nrf-2), which promotes the survival of cancer cells and cause NF-κB activation. NF-κB is involved in processes such as cell proliferation, invasion, and metastasis. By deactivating ROS, β-carotene helps protect brain cells from oncogenesis.[89] The absorption of β-carotene occurs in the human intestinal mucosa.[42] A portion of dietary β-carotene is transported with lipoproteins *via* the bloodstream to tissues, where it is metabolised or stored.[90] It is cleaved into β-apo-carotenals and all-trans-retinal, which is subsequently converted to retinol. Central cleavage to retinal is catalysed by β-carotene-15,15′-oxygenase enzymes (CMOI). β-Apocarotenals are produced after nonspecific cleavage at several double bonds, catalysed by CMOII enzymes.[47] Retinal may be converted into retinol, retinoic acid, and other polar metabolites, which are then transported to the bloodstream

Published on 04 July 2025. Downloaded on 5/25/2026 7:46:48 AM.

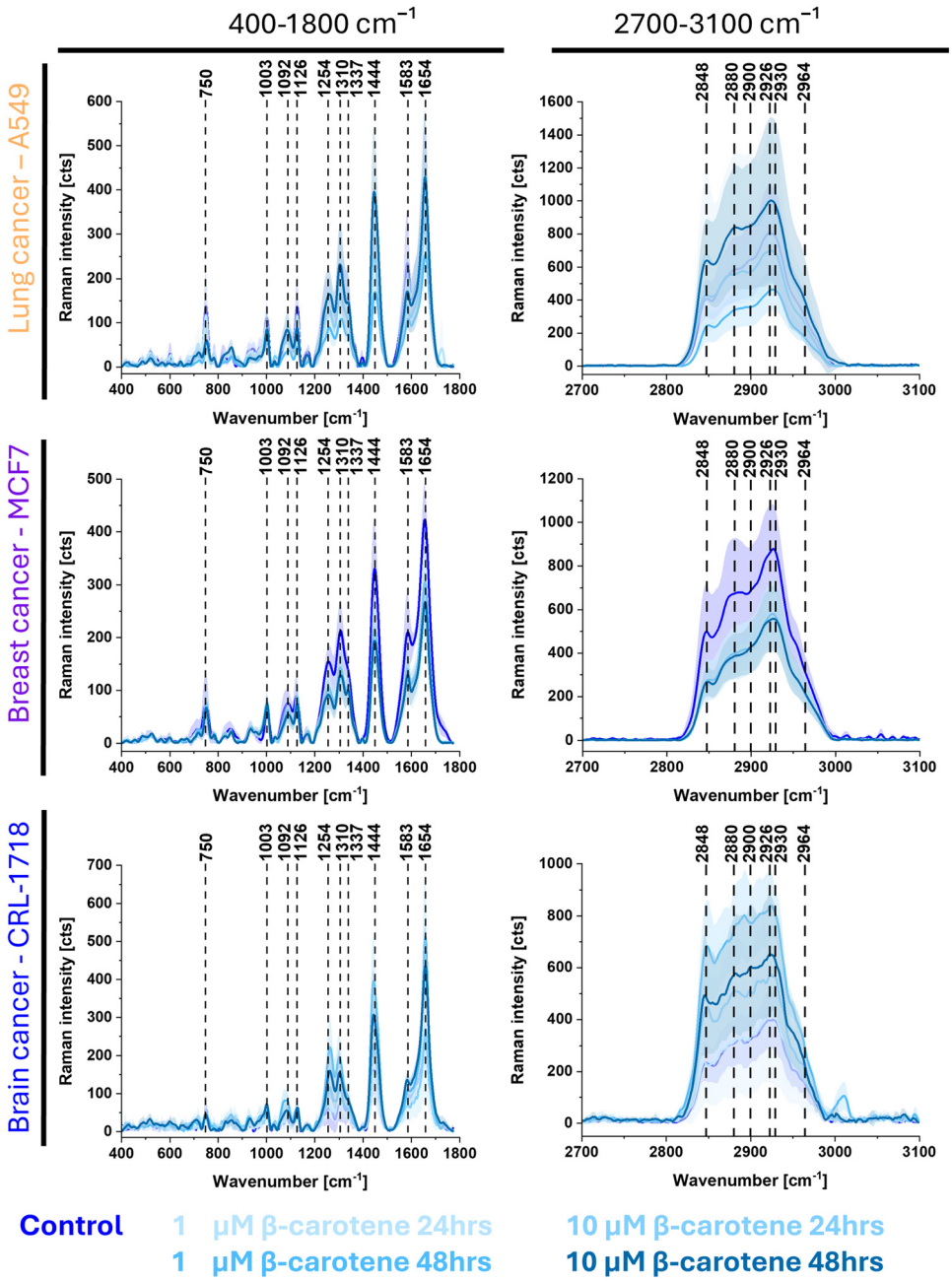

Fig. 4 Average Raman spectra in the ranges from 400 to 1800 cm^{-1} and from 2700 to 3100 cm^{-1} for lipid droplets/endoplasmic reticulum from A549 (orange), MCF7 (violet) and CRL-1718 (blue) cell lines. Colours on the spectra correspond to control cells and each variant of supplementation with β-carotene: 1 and 10 μM for 24 and 48 hours.

from intestinal mucosal cells.[42] Retinoic acid binds to retinoic acid receptors (RARs) and retinoid X receptors (RXRs), which are nuclear receptors involved in steroid hormone signalling.[91] Upon activating, these receptors modulate the expression of genes encoding proteins and enzymes. When retinoids bind to RARs, they stimulate the expression of genes involved in cell differentiation and apoptosis, and inhibit the metastasis of breast cancer.[92]

For a better understanding of the mechanisms of β-carotene action inside the cell, we prepared difference spectra for lipid droplets/endoplasmic reticulum, nucleus and mitochondria. Fig. 6–8 present difference spectra for lipid droplets/endoplasmic reticulum (Fig. 6), nucleus (Fig. 7), and mitochondria (Fig. 8) from lung, breast, and brain cells.

The Fig. 6 shows the boundary conditions (the control cells without supplementation and the higher β-carotene concentration with longer incubation time). It can be seen that in the lung cancer cells (A549) most of the bands have lower or the same intensity as the control cells, except for the band at 1444 cm^{-1}, which has a higher intensity. The intensities of all bands in lung cancer cells between 2700 and 3100 cm^{-1} are higher

 This journal is © the Owner Societies 2025

Published on 04 July 2025. Downloaded on 5/25/2026 7:46:48 AM.

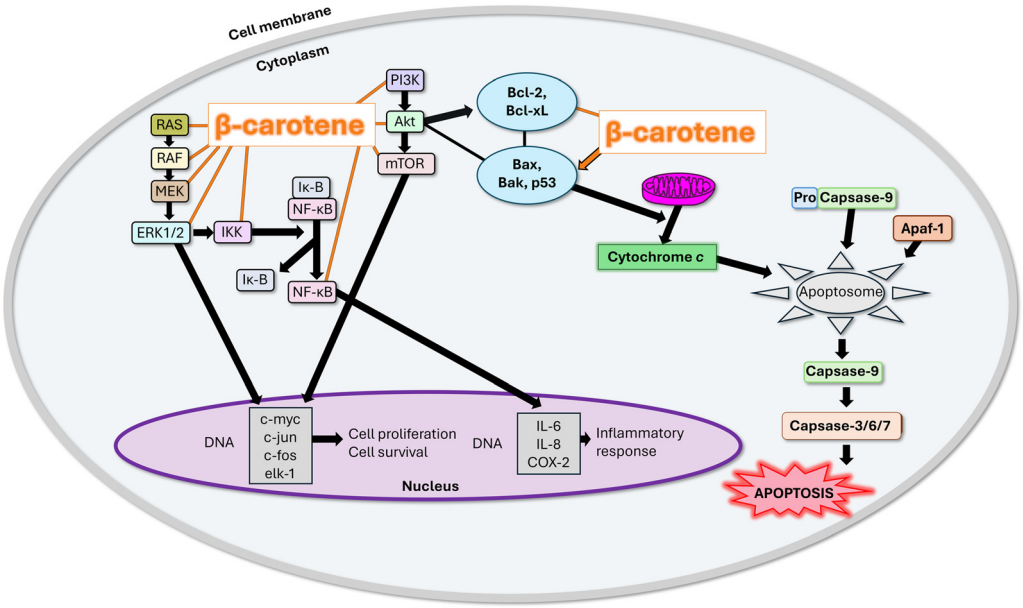

Fig. 5 The mechanism of β-carotene activity inside human cell.[82] Abbreviations: APAF-1 - apoptotic protease activating factor-1; Bak - Bcl-2 homologues antagonist/killer; BAX - Bcl-2 associated X; Bcl-2 - B-cell lymphoma 2; Bcl-XL - B-cell lymphoma-extra-large; c-*fos*, c-*jun*, c-*myc* – genes; COX-2 - cyclooxygenase 2; elk-1 - ETS transcription factor ELK1; ERK - extracellular signal-reduced kinase; IKK - inhibitory-κB kinase; Iκ-B -Ikappa-B kinase; IL-6; IL-8 - pro-inflammatory cytokines; MEK - mitogen-activated protein kinase/extracellular signal-reduced kinase; MOMP - mitochondrial outer membrane permeabilization; NF-κB - nuclear factor kappa-light-chain-enhancer of activated B cells; p38 MAPK - p38 mitogen-activated protein kinase; p53 - tumour protein; PI3K - phosphoinositide 3-kinase; RAF - member of the RAF kinase family; RAS - a guanosine-nucleotide-binding protein.

than in control cells. In breast cancer (MCF7), all intensities in both ranges are lower than in control cells, apart from protein band at 1003 cm^{-1}, which shows no significant changes. In the range from 400 to 1800 cm^{-1} in brain cancer cells (CRL-1718), most bands have lower or the same intensity as in control cells. The exception is the band at 1310 cm^{-1}, which has a higher intensity compared to control cells. In brain cancer, the band at 2848 cm^{-1} has the same intensity, the other bands have a lower intensity than control cells. This could mean that in lipid droplets of lung cells β-carotene increases the number of proteins and lipids (bands at 1444 and in the range of 2700 to 3100 cm^{-1}), in breast cells it decreases the number of cellular components, and in brain cells it also decreases the number of cellular components or makes them the same as in unsupplemented cells. Importantly, in lung and brain cancer, β-carotene supplementation resulted in lower band intensities at 750, 1126 and 1583 cm^{-1}. In breast cancer cells, the changes in band intensities at 750 and 1126 cm^{-1} were not evident, but the band intensity at 1583 cm^{-1} was lower than in control cells. This may indicate that β-carotene alters the redox state of cytochrome *c* in lipid droplets. Analogous analysis was conducted for cell nucleus (Fig. 7) and mitochondria (Fig. 8). Raman spectra of A549 cells after β-carotene supplementation showed higher intensities in the mitochondria, as in the lipid droplets/endoplasmic reticulum. However, in the nucleus, in 400–1800 cm^{-1} the intensity was slightly lower, and in 2700–3100 cm^{-1} there was almost no difference. After β-carotene supplementation, the difference in the Raman spectra of MCF7 cells showed lower intensities for all bands in the 400–1800 and 2700–3100 cm^{-1} spectral ranges in the nucleus and mitochondria, as in the lipid droplets/endoplasmic reticulum. CRL-1718 cells after β-carotene supplementation had higher intensities of all analysed bands in both spectral ranges for the nucleus and mitochondria. This was the opposite result to that obtained in lipid droplets. In the ESI,† we present normalized difference spectra corresponding to lipid droplets (Fig. S6, ESI†), nucleus (Fig. S7, ESI†), and mitochondria (Fig. S8, ESI†).

Focusing on the differences between each organ with and without supplementation, we present a partial least squares-discriminant analysis (PLS-DA). Fig. 9 shows plots of PLS-DA results for all recorded Raman spectra of brain, breast, and lung cancer cells before and after β-carotene supplementation.

Fig. 9 shows the PLS-DA results on control cells and cells supplemented with 10 μM β-carotene. In panel (C) we can see Raman spectra for each latent variable: LV1 (58.15%), LV2 (9.84%), LV3 (4.50%), LV4 (5.11%) and LV5 (4.51%). The following Raman bands can be distinguished on the spectra: 750, 1003, 1092, 1126, 1254, 1310, 1337, 1444, 1583 and 1654 cm^{-1}. LV1 represents most of the analysed data (58.15%) and includes the following bands at: 1003, 1254, 1310, 1337, 1444 and 1654 cm^{-1}. It can be assumed that most of the analysed data corresponds to lipids (1254, 1444, 1654 cm^{-1}) and proteins (1003, 1337, 1654 cm^{-1}). LV2–LV5 have different spectral patterns, but the main Raman bands at 750, 1003, 1126, 1254, 1310, 1337, 1444, 1583 and 1654 cm^{-1} can be distinguished. Although we also see bands from lipids and proteins in these spectra, bands from cytochrome *c* (750, 1126, 1310, 1583 cm^{-1}) are very prominent. This may indicate that

Published on 04 July 2025. Downloaded on 5/25/2026 7:46:48 AM.

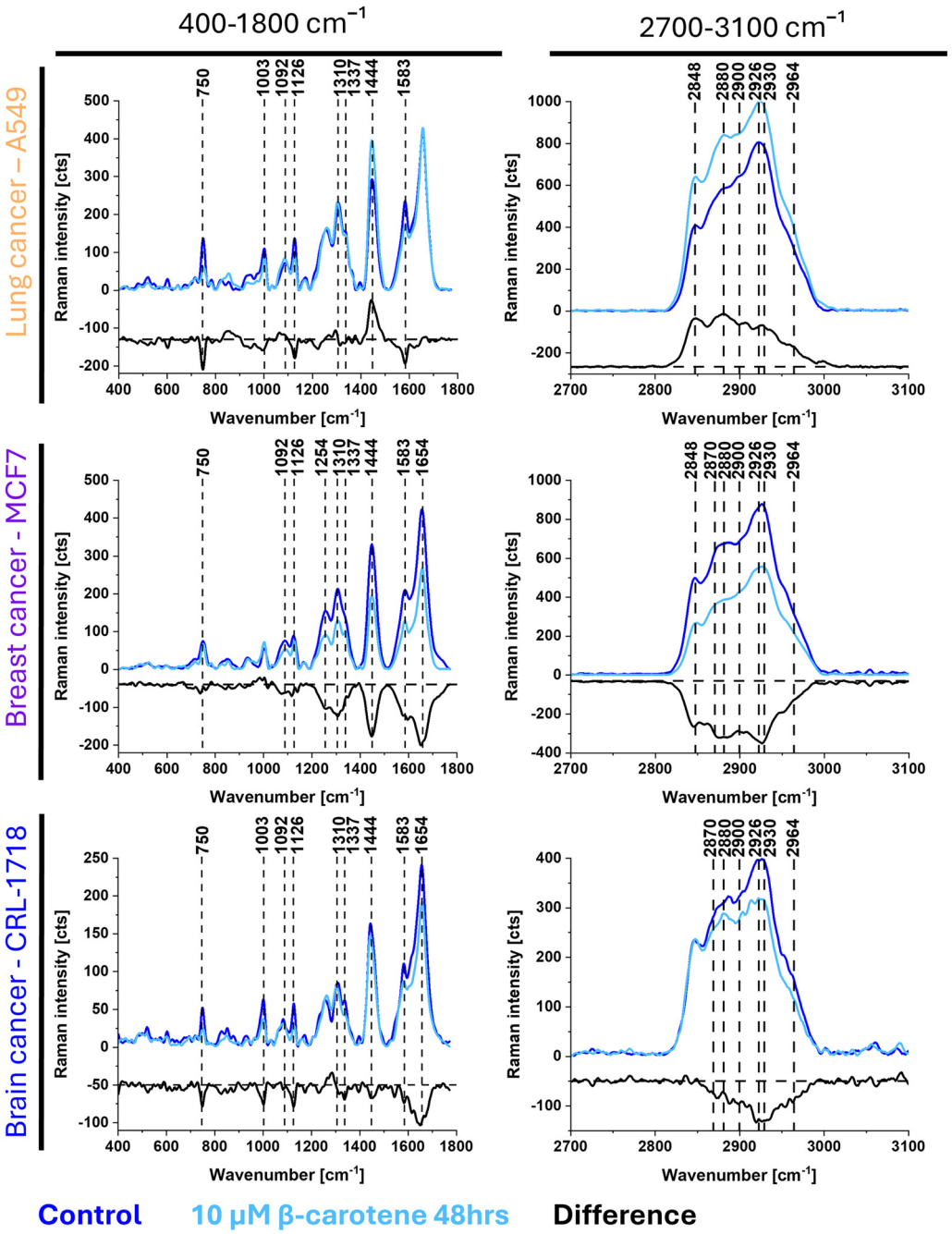

Fig. 6 Raman spectra of lipid droplets/endoplasmic reticulum in A549 (orange), MCF7 (violet) and CRL-1718 (blue) cell lines in range from 400 to 1800 cm^{-1} and 2700 to 3100 cm^{-1} and difference spectra. Colours on the panels correspond to control cells (blue), cells supplemented with 10 μM of β-carotene after 48 hours (light blue) and difference between them (black). The difference was calculated by subtracting the spectra of the control cells from those of the supplemented cells.

LV2–LV5 are a representation of the redox state of cytochrome *c*. The PLS-DA score plot shows a good separation between the three control classes (orange, violet and blue squares with black edges). We can also see the difference between control (squares) and supplemented (rhombuses) classes. The most isolated are the MCF7 controls located in the upper left corner of panel A. In addition, the A549 cell control class is also separated from the other classes. Therefore, the Raman data allowed us to distinguish non-supplemented cells from β-carotene-supplemented cells. The supplemented cells did not form three separate groups, they were mixed. This may indicate that β-carotene supplementation produced similar results in each organ on the cellular level. However, at the cell organelle level, the β-carotene supplementation caused different results in each analysed organ.

To illustrate statistically significant differences in individual Raman bands of cytochrome *c*, lipids, and proteins, which may be Raman biomarkers of cellular responses to β-carotene

 This journal is © the Owner Societies 2025

Published on 04 July 2025. Downloaded on 5/25/2026 7:46:48 AM.

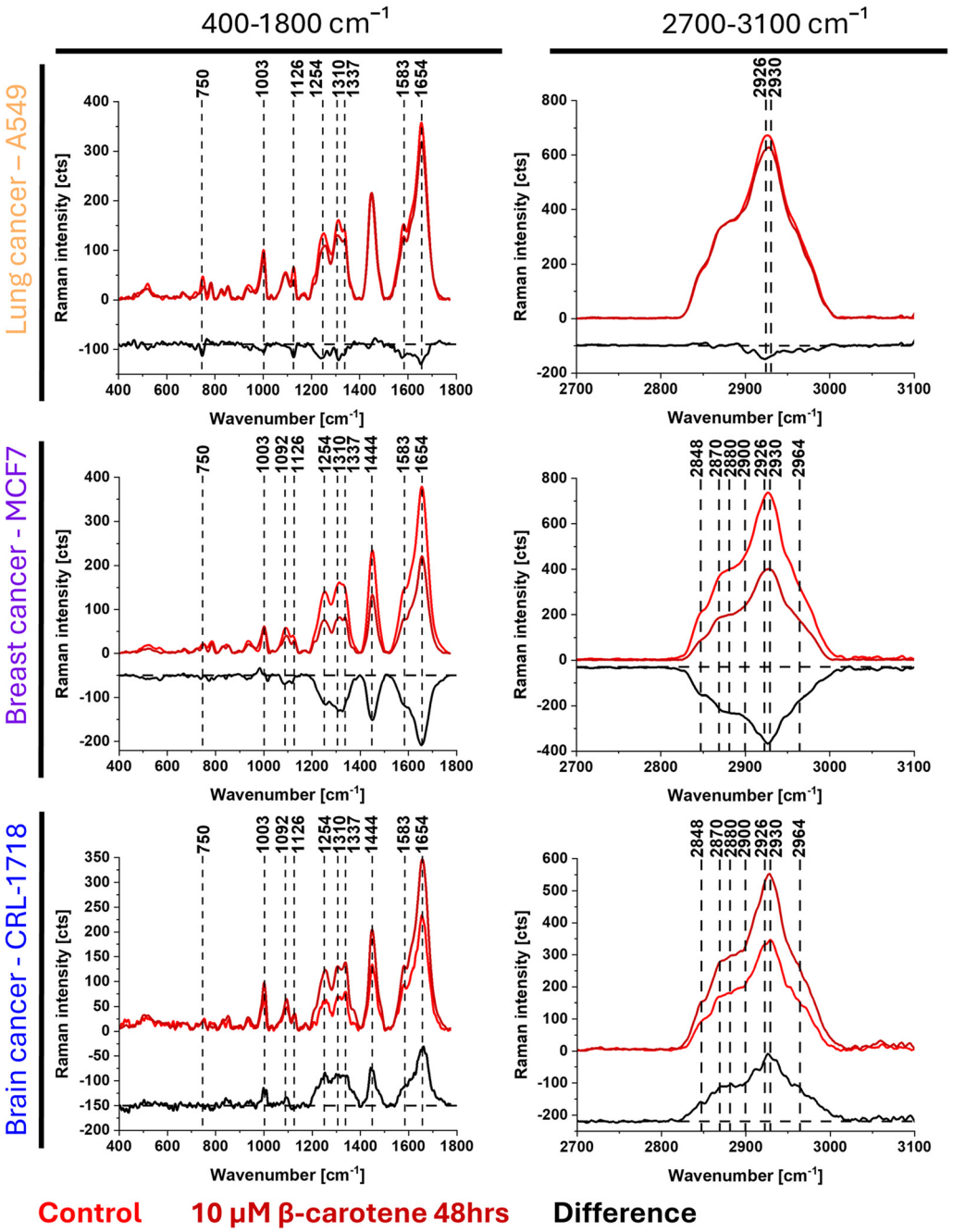

Fig. 7 Raman spectra of cell nucleus in A549 (orange), MCF7 (violet) and CRL-1718 (blue) cell lines in range from 400 to 1800 cm^{-1} and 2700 to 3100 cm^{-1} and difference spectra. Colours on the panels correspond to control cells (red), cells supplemented with 10 μM of β-carotene after 48 hours (dark red) and difference between them (black). The difference was calculated by subtracting the spectra of the control cells from those of the supplemented cells.

supplementation, we used a one-way ANOVA test. Fig. 10 shows the differences in the Raman bands of cytochrome *c* (750, 1126 cm^{-1}) and lipids (2848 cm^{-1}) in lipid droplets/endoplasmic reticulum. These differences occurred after β-carotene supplementation for 24 and 48 hours.

A one-way ANOVA with Tukey's test was performed to verify differences between control and supplemented cells, as well as between β-carotene doses and incubation time. We analysed lipid droplets/endoplasmic reticulum on Raman bands at 750, 1126 (cytochrome *c*) and 2848 (lipids) cm^{-1}. In all bands, significant differences were found between control and supplemented cells and between β-carotene concentrations (doses), except for the band at 1126 cm^{-1} in lung cancer cells and 2848 cm^{-1} in breast cancer cells, where differences only occurred between control and supplemented cells. In all cases analysed, there were differences at both incubation times, except for the band at 750 cm^{-1} in breast cancer cells, where differences only occurred after 24 hours of incubation. This suggests that β-carotene supplementation modifies cellular metabolism in lipid droplet organelles, alters the redox state

Published on 04 July 2025. Downloaded on 5/25/2026 7:46:48 AM.

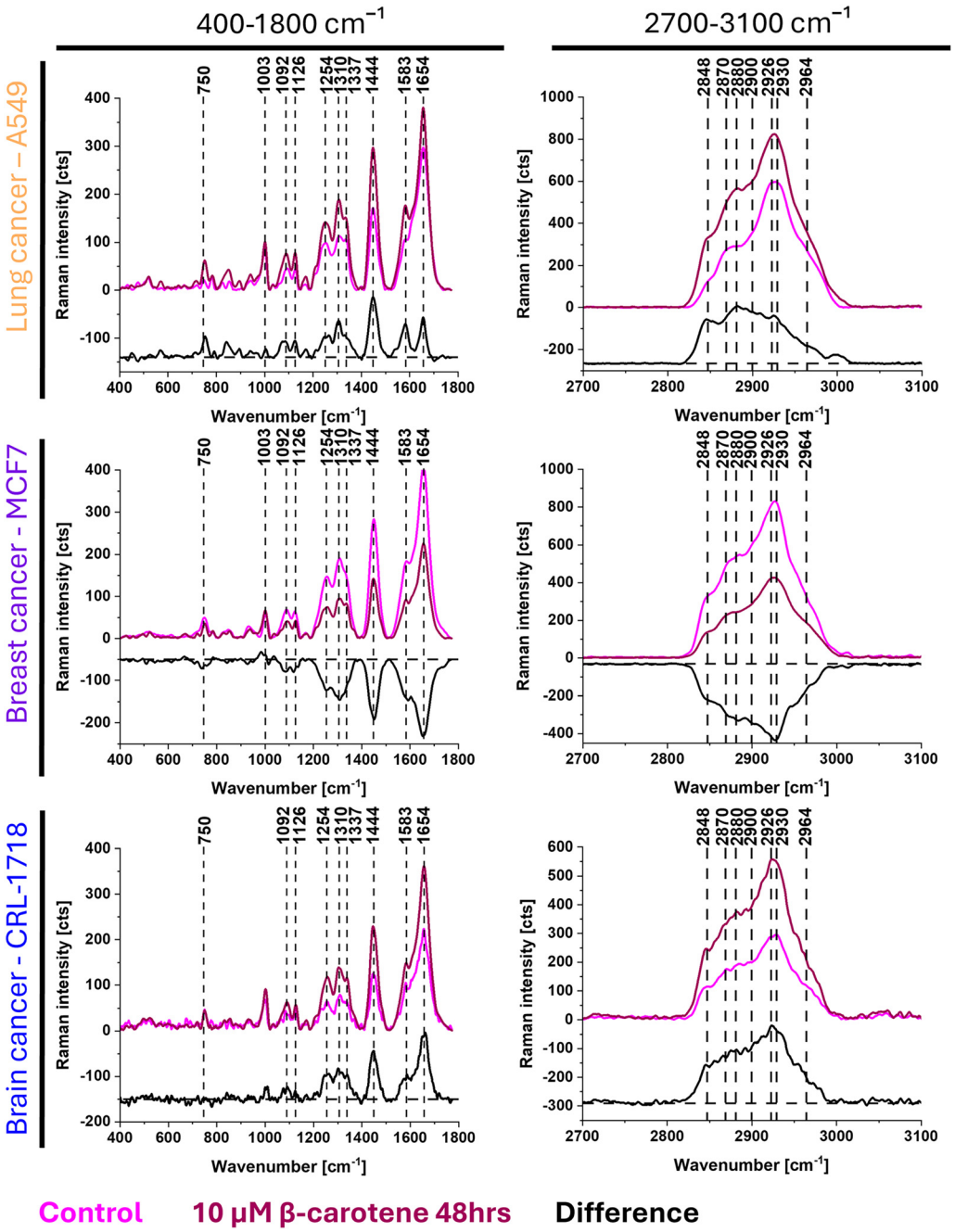

Fig. 8 Raman spectra of cell mitochondria in A549 (orange), MCF7 (violet) and CRL-1718 (blue) cell lines in range from 400 to 1800 cm^{-1} and 2700 to 3100 cm^{-1} and difference spectra. Colours on the panels correspond to control cells (magenta), cells supplemented with 10 μM of β-carotene after 48 hours (dark pink) and difference between them (black). The difference was calculated by subtracting the spectra of the control cells from those of the supplemented cells.

of cytochrome *c* and the amount of lipids significantly depending on supplementation or lack of there, β-carotene dose, and incubation time with β-carotene.

The results presented so far have shown changes in lung (A549), breast (MCF7) and brain (CRL-1718) cancer cells after β-carotene supplementation. Furthermore, we have demonstrated that Raman imaging is an excellent tool for label-free monitoring of tumour metabolism at the cellular level. In lung cancer cells, β-carotene increased the intensities of bands corresponding to lipids (1444, 2848 cm^{-1}) and lipids/proteins (bands at 2880–2964 cm^{-1}). Furthermore, the intensity of bands at 750, 1126, 1583 cm^{-1} was lower after supplementation than in control cells, indicating that β-carotene altered the redox state of cytochrome *c* in lipid droplets in lung cancer cells. In breast cancer cells, β-carotene supplementation resulted in a lower intensity of all Raman bands, which may indicate that β-carotene inhibits cellular metabolism in lipid droplets and therefore the amount of most cellular components

 This journal is © the Owner Societies 2025

Published on 04 July 2025. Downloaded on 5/25/2026 7:46:48 AM.

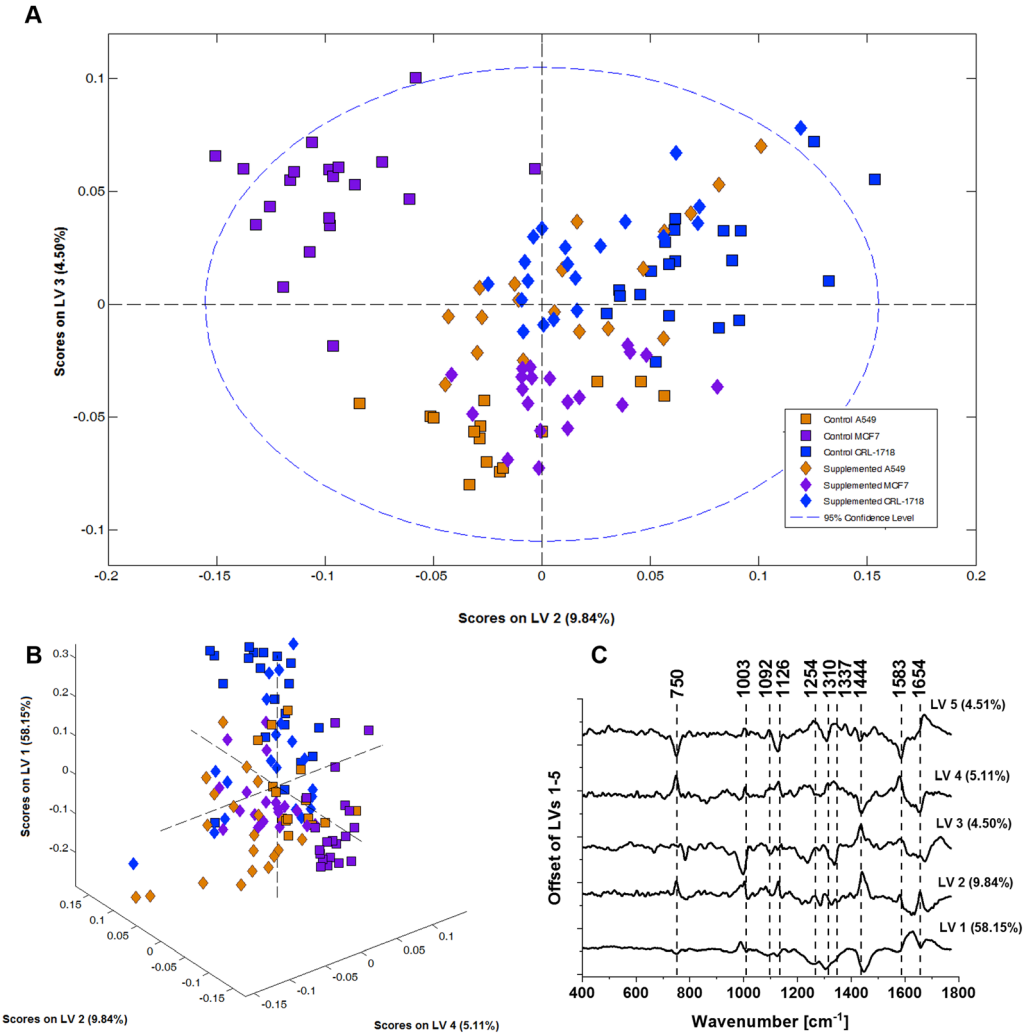

Fig. 9 PLS-DA score plots (model mean centre): (A) – LV2 *vs.* LV3, (B) – LV4 *vs.* LV2 *vs.* LV1 for Raman spectra of control cells: A549 (orange square with black edges), MCF7 (violet square with black edges), CRL-1718 (blue square with black edges) and supplemented with β-carotene: A549 (orange), MCF7 (violet), CRL-1718 (blue). The plots of latent variables (LV1–5) in low frequency region are presented in panel (C).

is lower than in control cells. In lipid droplets of brain cancer cells, the addition of β-carotene decreased the intensity of most bands, except for an increase in the intensity of the band at 1310 cm^{-1}, which corresponds to mixed fat chains (lipids), and maintained the intensity of the band at 2848 cm^{-1}. Thus, β-carotene can inhibit the growth of brain cancer cells, but to a lesser extent than in breast cancer cells. These results generally show that β-carotene alters the metabolism of a single cell, especially in lipid droplets/endoplasmic reticulum, and that this alteration is different in lung, breast, and brain cancer cells.

We found that β-carotene supplementation increased the amount of lipids in lipid droplets of human lung cancer cells, which may be related to a redirection of cellular metabolism to lipid overproduction. This is an unconventional finding, as β-carotene has been labelled effective in cancer prevention, the only exception being the smoking group, where β-carotene increased lung cancer development.[93,94] Our results agree with Wright *et al.* who found the molecular origin of this effect. They suggested that β-carotene supplementation results in aberrant cell growth.[95] Some studies have shown that even if β-carotene induces cancer development in smokers, it has a beneficial effect on non-smokers.[84] If our results can be understood as an increase in cancer development, this would be consistent with Jeon *et al.* who found that β-carotene supplementation did not express a preventive effect on cancer incidence and cancer mortality.[96] Our findings agree with Kordiak *et al.* who claimed that β-carotene supplementation increased the risk of lung cancer.[97] They analysed clinical trials on lung cancer risk. Ruano-Ravina *et al.* analysed the effects of carotenoids and vitamins on the development of lung cancer and found that β-carotene alone did not prevent this cancer.[98] In contrast to our findings, Yu *et al.* has showed that higher diet β-carotene and vitamin A intake reduce the risk of lung cancer.[99] Another example of the opposite of our results is the research of Shareck *et al.*[100] They analysed clinical trials and found that β-carotene has preventive influence on lung cancer. However, the anti-cancer properties of β-carotene were due to its antioxidant function.

Published on 04 July 2025. Downloaded on 5/25/2026 7:46:48 AM.

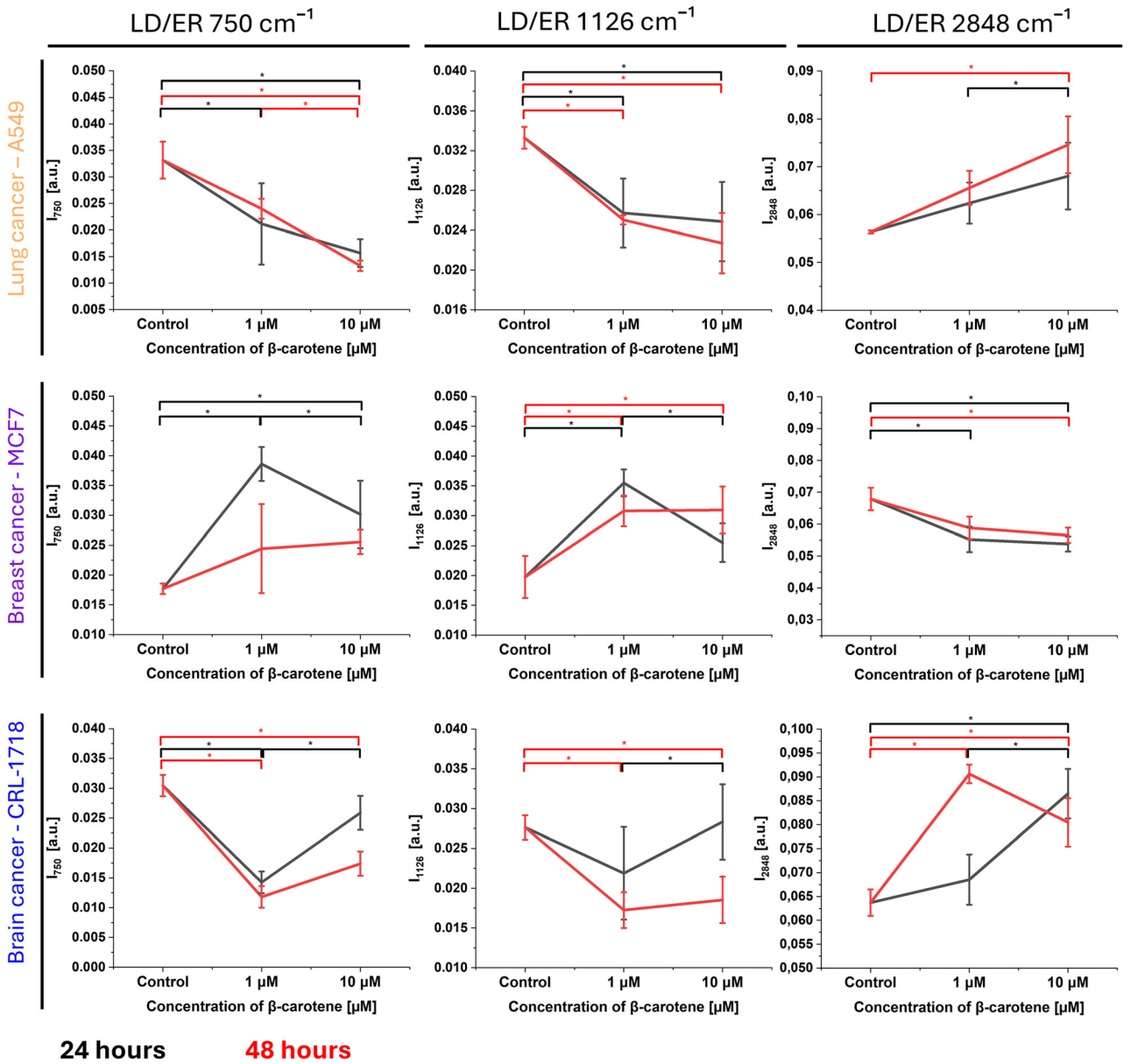

Fig. 10 Differences in the Raman bands at 750, 1126 and 2848 cm^{-1} peak intensity and standard deviation (SD) for lipid droplets/endoplasmic reticulum in A549 (orange), MCF7 (violet) and CRL-1718 (blue) cells. Points represent control cells and cells supplemented with β-carotene (1 and 10 μM). The black line refers to 24 and red line to 48 hours supplementation.

Our findings on the effects of β-carotene on breast and brain cancer cells are similar. We found that β-carotene acts on these cancers by reducing the amount of most cellular components, such as lipids (Raman bands at 1254, 1444, 2848 cm^{-1}) or proteins (Raman bands at 1003, 1310, 2880–2964 cm^{-1}) in lipid droplets. Our results agree with Gloria *et al.*[87] who found that β-carotene supplementation induces cell cycle arrest and apoptosis in human breast cancer. They also studied MCF7 cells and proved by MTT assays that β-carotene supplementation induces apoptosis. This could be biological evidence for our findings. Another biological proof was provided by Sowmya-Shree *et al.*[101] who claimed that β-carotene increased apoptosis in MCF7 cells, which was associated to increased capsase-3 activity. In opposition to our research results stands Nagel *et al.* who claimed that β-carotene has weak protective effect.[102] They analysed data from clinical trials. We analysed the influence of all-*trans*-retinal (ALTR) on brain cancer cells and found that ALTR as a metabolite of β-carotene inhibits brain cancer development.[54] Our results have proven that β-carotene supplementation changes human metabolism on the cellular level. It agrees with Kim *et al.* who analysed neuroblastoma and proved that β-carotene inhibits cell invasion and metastasis by decreasing the level of hypoxia-inducible factor-1α.[103] Holick *et al.*[104] stands in opposition to our results. They claim that carotenoid consumption is not likely associated with the risk of adult glioma. Lin *et al.* also claimed that β-carotene

 This journal is © the Owner Societies 2025

Published on 04 July 2025. Downloaded on 5/25/2026 7:46:48 AM.

intake does not benefit the incidence or mortality of brain cancer.[105] However, β-carotene has a confirmed influence on brain diseases like Alzheimer's.[106] Thus, it is proven that β-carotene affects brain cells. In summary, the mechanism of action varies on the organ.

Conclusions

Here, we employed Raman spectroscopy to analyse the potential impact of β-carotene on lung, breast, and brain cancer cells in the context of cancer prevention. Our results revealed organ-specific effects: β-carotene enhanced lipid production in lung cancer cells, as evidenced by changes in the intensity of lipid-associated Raman bands (1444, 2848 cm^{-1}). Conversely, it inhibited cell growth and reduced lipid and protein levels in breast and brain cancer cells, demonstrated by decreased intensities in Raman bands associated with lipids and proteins (1003, 1254, 1310, 1444, 1654, 2848–2964 cm^{-1}).

In summary, the results of this study highlight the organ-specific effects of β-carotene on cancer cell metabolism, suggesting its potential role in cancer prevention and treatment.

In the context of the current state of knowledge on the effects of β-carotene on human lung, breast, and brain cancer, we have demonstrated by Raman imaging that β-carotene modifies the metabolism in cancer cells. This study involved recording Raman spectra and images in human lung (A549), breast (MCF7) and brain (CRL-1718) cancer cells *in vitro* with and without β-carotene at concentrations of 1 and 10 μM after 24 and 48 hours of incubation. Therefore, we demonstrated that Raman imaging is an effective technique for qualitative and quantitative analysis of individual cellular organelles. We found that β-carotene modifies the functional activity of cells, causing changes in lipids, proteins, and redox state of cytochrome *c*. We focused on lipid droplets and demonstrated that in this cell organelle, β-carotene supplementation improves the amount of lipids in proteins in lung cancer, reduces the amount of lipids and proteins in breast cancer, and mainly reduces the amount of lipids and proteins in brain cancer. An important finding is that β-carotene altered the redox state of cytochrome *c* (bands at 750, 1126 and 1583 cm^{-1}) in lipid droplets. These findings provide promising support for understanding the effects of β-carotene on three common human cancers - lung, breast, and brain.

Author contributions

Conceptualization: K. J., J. S.; investigation: K. J.; methodology: J. S.; writing – original draft: K. J., J. S.; manuscript editing: J. S., K. J.; M. K. manuscript revision: J. S., M. K., K. J. All authors have read and agreed to the published version of the manuscript.

Conflicts of interest

There are no conflicts of interest to declare.

Data availability

The data supporting this article have been included as part of the ESI.†

Acknowledgements

This work was supported by the FU^2N – Young Scientists' Skills Improvement Fund, Grant: ''Application of Raman spectroscopy in the analysis of carotenoid-supplemented cancer cells-determining the impact.'' Number 503/3-34-4-1 and the National Science Centre of Poland (OPUS, UMO 2021/43/B/ST4/01547). This paper has been completed while the first author was the Doctoral Candidate in the Interdisciplinary Doctoral School at the Lodz University of Technology, Poland. The research was supported by the Statutory Funding.

References

1 R. L. Siegel, A. N. Giaquinto and A. Jemal, Cancer statistics, 2024, *CA. Cancer J. Clin.*, 2024, **74**, 12–49.
2 S. K. N. Marie and S. M. O. Shinjo, Metabolism and Brain Cancer, *Clinics*, 2011, **66**, 33–43.
3 M. Kopeć, K. Beton, K. Jarczewska and H. Abramczyk, Hyperglycemia and cancer in human lung carcinoma by means of Raman spectroscopy and imaging, *Sci. Rep.*, 2022, **12**, 18561.
4 L. A. Torre, R. L. Siegel and A. Jemal, *Lung Cancer Statistics*, Advances in Experimental Medicine and Biology, 2016, vol. 893, pp. 1–19.
5 M. B. Schabath and M. L. Cote, Cancer Progress and Priorities: Lung Cancer, *Cancer Epidemiol., Biomarkers Prev.*, 2019, **28**, 1563–1579.
6 K. C. Thandra, A. Barsouk, K. Saginala, J. S. Aluru and A. Barsouk, Epidemiology of lung cancer, *Contemp. Oncol.*, 2021, **25**, 45–52.
7 J. D. Minna, J. A. Roth and A. F. Gazdar, Focus on lung cancer, *Cancer Cell*, 2002, **1**, 49–52.
8 K. M. Fong, Y. Sekido and J. D. Minna, The Molecular Basis of Lung Carcinogenesis. in *The Molecular Basis of Human Cancer* ed. W. B. Coleman and G. J. Tsongalis, Humana Press, Totowa, NJ, 2002, pp. 379–405, DOI: **10.1007/978-1-59259-125-1_17**.
9 W. D. Travis, *et al.*, International association for the study of lung cancer/american thoracic society/european respiratory society international multidisciplinary classification of lung adenocarcinoma, *J. Thorac. Oncol.*, 2011, **6**, 244–285.
10 L. G. Collins, C. Haines, R. Perkel and R. E. Enck, Lung Cancer: Diagnosis and Management, *Am. Fam. Physician*, 2007, **75**, 56–63.
11 W. D. Travis, Pathology of Lung Cancer, *Clin. Chest Med.*, 2011, **32**, 669–692.
12 M.-H. Tao, Epidemiology of lung cancer. in *Lung Cancer and Imaging*, IOP Publishing, 2019, DOI: **10.1088/978-0-7503-2540-0ch4**.

Published on 04 July 2025. Downloaded on 5/25/2026 7:46:48 AM.

13 S. J. Adams, *et al.*, Lung cancer screening, *Lancet*, 2023, **401**, 390–408.
14 M. E. Monaco, Fatty acid metabolism in breast cancer subtypes, *Oncotarget*, 2017, **8**, 29487–29500.
15 M. Cazzaniga and B. Bonanni, Breast Cancer Metabolism and Mitochondrial Activity: The Possibility of Chemoprevention with Metformin, *BioMed Res. Int.*, 2015, **2015**, 972193.
16 B. A. Gusterson and T. Stein, Human breast development, *Semin. Cell Dev. Biol.*, 2012, **23**, 567–573.
17 Y.-S. Sun, *et al.*, Risk Factors and Preventions of Breast Cancer, *Int. J. Biol. Sci.*, 2017, **13**, 1387–1397.
18 Z. Momenimovahed and H. Salehiniya, Epidemiological characteristics of and risk factors for breast cancer in the world, *Breast Cancer Targets Ther.*, 2019, **11**, 151–164.
19 N. Karssemeijer, *et al.*, Breast Cancer Screening Results 5 Years after Introduction of Digital Mammography in a Population-based Screening Program, *Radiology*, 2009, **253**, 353–358.
20 M. S. Gazzaniga, Organization of the Human Brain, *Science*, 1989, **245**, 947–952.
21 R. Free, J. Clark, S. Amara and D. R. Sibley, Neurotransmission in the Central Nervous System, in *Goodman & Gilman's: The Pharmacological Basis of Therapeutics, 13e*, ed. L. L. Brunton, R. Hilal-Dandan and B. C. Knollmann, McGraw-Hill Education, 2017, **https://accessmedicine.mhmedical.com/content.aspx?bookid=2189&sectionid=170349771**.
22 P. Brodal, *The Central Nervous System*, Oxford University Press, 2010.
23 J. Salas-Salvadó, M. Á. Martinez-González, M. Bulló and E. Ros, The role of diet in the prevention of type 2 diabetes, *Nutr., Metab. Cardiovasc. Dis.*, 2011, **21**, B32–B48.
24 C. Liang, K. DeCourcy and M. R. Prater, High–saturated-fat diet induces gestational diabetes and placental vasculopathy in C57BL/6 mice, *Metabolism*, 2010, **59**, 943–950.
25 A. M. Hodge, M. N. Karim, J. R. Hébert, N. Shivappa and B. de Courten, Association between Diet Quality Indices and Incidence of Type 2 Diabetes in the Melbourne Collaborative Cohort Study, *Nutrients*, 2021, **13**, 4162.
26 V. Lazar, L.-M. Ditu, G. G. Pircalabioru, A. Picu, L. Petcu, N. Cucu and M. C. Chifiriuc, Gut Microbiota, Host Organism, and Diet Trialogue in Diabetes and Obesity, *Front. Nutr.*, 2019, **6**, 21.
27 M. Verboven, D. Deluyker, D. Hansen, B. O. Eijnde and V. Bito, P1463The origin of diabetes: high-sugar diet to induce diabetic cardiomyopathy in rats, *Eur. Heart J.*, 2017, **38**, ehx502.P1463.
28 K. Lim, B. Barzel, S. L. Burke, J. A. Armitage and G. A. Head, Origin of Aberrant Blood Pressure and Sympathetic Regulation in Diet-Induced Obesity, *Hypertension*, 2016, **68**, 491–500.
29 N. Hariri and L. Thibault, High-fat diet-induced obesity in animal models, *Nutr. Res. Rev.*, 2010, **23**, 270–299.
30 L. D. Ruiz, M. L. Zuelch, S. M. Dimitratos and R. E. Scherr, Adolescent Obesity: Diet Quality, Psychosocial Health, and Cardiometabolic Risk Factors, *Nutrients*, 2020, **12**, 43.
31 P. Huypens, *et al.*, Epigenetic germline inheritance of diet-induced obesity and insulin resistance, *Nat. Genet.*, 2016, **48**, 497–499.
32 A. Mente, *et al.*, Diet, cardiovascular disease, and mortality in 80 countries, *Eur. Heart J.*, 2023, **44**, 2560–2579.
33 C. Cooper, *et al.*, Review: developmental origins of osteoporotic fracture, *Osteoporos. Int.*, 2006, **17**, 337–347.
34 B. Teucher and S. Fairweather-Tait, Dietary sodium as a risk factor for osteoporosis: where is the evidence?, *Proc. Nutr. Soc.*, 2003, **62**, 859–866.
35 M. Martiniakova, *et al.*, The Role of Macronutrients, Micronutrients and Flavonoid Polyphenols in the Prevention and Treatment of Osteoporosis, *Nutrients*, 2022, **14**, 523.
36 D. A. Nelson, Evolutionary Origins of the Differences in Osteoporosis Risk in US Populations, *J. Clin. Densitom.*, 2019, **22**, 301–304.
37 S.-C. Chuang, *et al.*, Diet and the risk of head and neck cancer: a pooled analysis in the INHANCE consortium, *Cancer, Causes Control, Pap. Symp.*, 2012, **23**, 69–88.
38 C. Sapienza and J.-P. Issa, Diet, Nutrition, and Cancer Epigenetics, *Annu. Rev. Nutr.*, 2016, **36**, 665–681.
39 M. C. Stern, J. Barnoya, J. P. Elder and K. Gallegos-Carrillo, Diet, physical activity, obesity and related cancer risk: strategies to reduce cancer burden in the Americas, *Rev. Invest. Salud Publica*, 2020, **61**, 448–455.
40 H. Marona, A. Gunia and E. Pękala, *Retinoidy – rola w farmakoterapii w aspekcie komórkowego mechanizmu działania*, 2010.
41 S. Agarwal and A. V. Rao, Carotenoids and chronic diseases, *Drug Metabol. Drug Interact.*, 2000, **17**, 189–210.
42 X. D. Wang, Review: absorption and metabolism of beta-carotene, *J. Am. Coll. Nutr.*, 1994, **13**, 314–325.
43 D. A. Hughes, Effects of carotenoids on human immune function, *Proc. Nutr. Soc.*, 1999, **58**, 713–718.
44 H. Stähelin, K. Gey, M. Eichholzer and E. Lüdin, *β*-Carotene and cancer prevention: the Basel Study, *Am. J. Clin. Nutr.*, 1991, **53**, 265S–269S.
45 N. Druesne-Pecollo, *et al.*, Beta-carotene supplementation and cancer risk: a systematic review and metaanalysis of randomized controlled trials, *Int. J. Cancer*, 2010, **127**, 172–184.
46 G. van Poppel and R. Goldbohm, Epidemiologic evidence for beta-carotene and cancer prevention, *Am. J. Clin. Nutr.*, 1995, **62**, 1393S–1402S.
47 V. Shete and L. Quadro, Mammalian Metabolism of β-Carotene: Gaps in Knowledge, *Nutrients*, 2013, **5**, 4849–4868.
48 R. S. Parker, Absorption, metabolism, and transport of carotenoids, *FASEB J.*, 1996, **10**, 542–551.
49 H. Stutz, N. Bresgen and P. M. Eckl, Analytical tools for the analysis of β-carotene and its degradation products, *Free Radic. Res.*, 2015, **49**, 650–680.
50 V. E. de Oliveira, H. V. Castro, H. G. M. Edwards and L. F. C. de Oliveira, Carotenes and carotenoids in natural biological samples: a Raman spectroscopic analysis, *J. Raman Spectrosc.*, 2010, **41**, 642–650.

 This journal is © the Owner Societies 2025

Published on 04 July 2025. Downloaded on 5/25/2026 7:46:48 AM.

51 R. Withnall, B. Z. Chowdhry, J. Silver, H. G. M. Edwards and L. F. C. de Oliveira, Raman spectra of carotenoids in natural products, *Spectrochim. Acta, Part A*, 2003, **59**, 2207–2212.
52 M. Baranska, M. Roman, J. Cz. Dobrowolski, H. Schulz and R. Baranski, Recent Advances in Raman Analysis of Plants: Alkaloids, Carotenoids, and Polyacetylenes, *Curr. Anal. Chem.*, 2013, **9**, 108–127.
53 C. P. Marshall and A. Olcott Marshall, The potential of Raman spectroscopy for the analysis of diagenetically transformed carotenoids, *Philos. Trans. R. Soc., A*, 2010, **368**, 3137–3144.
54 K. Jarczewska, M. Kopeć, H. Abramczyk and J. M. Surmacki, Monitoring alterations of all-trans-retinal in human brain cancer cells by label-free confocal Raman imaging: regulation of the redox status of cytochrome *c*, *RSC Adv.*, 2024, **14**, 20982–20991.
55 Z. Movasaghi, S. Rehman and I. U. Rehman, Raman Spectroscopy of Biological Tissues, *Appl. Spectrosc. Rev.*, 2007, **42**, 493–541.
56 J. Conroy, A. G. Ryder, M. N. Leger, K. Hennessey and M. G. Madden, Qualitative and quantitative analysis of chlorinated solvents using Raman spectroscopy and machine learning, *Opto-Ireland 2005: Optical Sensing and Spectroscopy*, SPIE, 2005, vol. 5826, pp. 131–142.
57 K. A. Antonio and Z. D. Schultz, Advances in Biomedical Raman Microscopy, *Anal. Chem.*, 2014, **86**, 30–46.
58 E. E. Lawson, B. W. Barry, A. C. Williams and H. G. M. Edwards, Biomedical Applications of Raman Spectroscopy, *J. Raman Spectrosc.*, 1997, **28**, 111–117.
59 B. Brozek-Pluska, J. Musial, R. Kordek and H. Abramczyk, Analysis of Human Colon by Raman Spectroscopy and Imaging-Elucidation of Biochemical Changes in Carcinogenesis, *Int. J. Mol. Sci.*, 2019, **20**, 3398.
60 K. Jarczewska, M. Kopeć and J. M. Surmacki, Monitoring cellular human breast adenocarcinoma cells' response to xanthophylls by label-free Raman spectroscopy and imaging, *Spectrochim. Acta, Part A*, 2025, **339**, 126263.
61 K. Jarczewska, M. Kopeć and J. M. Surmacki, Raman signatures of astrocytoma metabolism alterations induced by crocin, fucoxanthin and lutein, *Spectrochim. Acta, Part A*, 2025, **342**, 126465.
62 J. Binoy, *et al.*, NIR-FT Raman and FT-IR spectral studies and ab initio calculations of the anti-cancer drug combretastatin-A4, *J. Raman Spectrosc.*, 2004, **35**, 939–946.
63 J. W. Chan, *et al.*, Micro-Raman spectroscopy detects individual neoplastic and normal hematopoietic cells, *Biophys. J.*, 2006, **90**, 648–656.
64 W.-T. Cheng, M.-T. Liu, H.-N. Liu and S.-Y. Lin, Micro-Raman spectroscopy used to identify and grade human skin pilomatrixoma, *Microsc. Res. Tech.*, 2005, **68**, 75–79.
65 R. K. Dukor, Vibrational Spectroscopy in the Detection of Cancer, in *Handbook of Vibrational Spectroscopy*, John Wiley & Sons, Ltd, 2006, DOI: 10.1002/0470027320.s8107.
66 A. J. Ruiz-Chica, M. A. Medina, F. Sánchez-Jiménez and F. J. Ramírez, Characterization by Raman spectroscopy of conformational changes on guanine–cytosine and adenine–thymine oligonucleotides induced by aminooxy analogues of spermidine, *J. Raman Spectrosc.*, 2004, **35**, 93–100.
67 G. Shetty, C. Kendall, N. Shepherd, N. Stone and H. Barr, Raman spectroscopy: elucidation of biochemical changes in carcinogenesis of oesophagus, *Br. J. Cancer*, 2006, **94**, 1460–1464.
68 D. Naumann, Infrared and NIR Raman spectroscopy in medical microbiology, *Proceedings*, 1998, **3257**, 245–257.
69 Z. Huang, *et al.*, Effect of formalin fixation on the near-infrared Raman spectroscopy of normal and cancerous human bronchial tissues, *Int. J. Oncol.*, 2003, **23**, 649–655.
70 L. Silveira Jr., *et al.*, Correlation between near-infrared Raman spectroscopy and the histopathological analysis of atherosclerosis in human coronary arteries, *Lasers Surg. Med.*, 2002, **30**, 290–297.
71 D. P. Lau, *et al.*, Raman spectroscopy for optical diagnosis in normal and cancerous tissue of the nasopharynx-preliminary findings, *Lasers Surg. Med.*, 2003, **32**, 210–214.
72 H. Abramczyk, B. Brozek-Pluska and M. Kopeć, Double face of cytochrome *c* in cancers by Raman imaging, *Sci. Rep.*, 2022, **12**, 2120.
73 C. J. Frank, R. L. McCreery and D. C. Redd, Raman spectroscopy of normal and diseased human breast tissues, *Anal. Chem.*, 1995, **67**, 777–783.
74 A. Haka, *et al.*, Haka AS, Shafer-Peltier KE, Fitzmaurice M, Crowe J, Dasari RR, Feld MSIdentifying microcalcifications in benign and malignant breast lesions by probing differences in their chemical composition using Raman spectroscopy, *Cancer Res.*, 2002, **62**, 5375–5380.
75 N. Stone, C. Kendall, J. Smith, P. Crow and H. Barr, Raman spectroscopy for identification of epithelial cancers, *Faraday Discuss.*, 2004, **126**, 141–157.
76 S. Koljenović, T. B. Schut, A. Vincent, J. M. Kros and G. J. Puppels, Detection of meningioma in dura mater by Raman spectroscopy, *Anal. Chem.*, 2005, **77**, 7958–7965.
77 N. J. Kline and P. J. Treado, Raman Chemical Imaging of Breast Tissue, *J. Raman Spectrosc.*, 1997, **28**, 119–124.
78 P. J. Caspers, G. W. Lucassen, E. A. Carter, H. A. Bruining and G. J. Puppels, In vivo confocal Raman microspectroscopy of the skin: noninvasive determination of molecular concentration profiles, *J. Invest. Dermatol.*, 2001, **116**, 434–442.
79 H. Abramczyk, *et al.*, Epigenetic changes in cancer by Raman imaging, fluorescence imaging, AFM and scanning near-field optical microscopy (SNOM). Acetylation in normal and human cancer breast cells MCF10A, MCF7 and MDA-MB-231, *Analyst*, 2016, **141**, 5646–5658.
80 C. S. B. Teixeira, *et al.*, Thyroid tissue analysis through Raman spectroscopy, *Analyst*, 2009, **134**, 2361–2370.
81 J. Rau, *et al.*, RAMAN spectroscopy imaging improves the diagnosis of papillary thyroid carcinoma, *Sci. Rep.*, 2016, **6**, 35117.
82 J. A. Kim, J.-H. Jang and S.-Y. Lee, An Updated Comprehensive Review on Vitamin A and Carotenoids in Breast

Published on 04 July 2025. Downloaded on 5/25/2026 7:46:48 AM.

Cancer: Mechanisms, Genetics, Assessment, Current Evidence, and Future Clinical Implications, *Nutrients*, 2021, **13**, 3162.
83 R. Sathasivam and J.-S. Ki, A Review of the Biological Activities of Microalgal Carotenoids and Their Potential Use in Healthcare and Cosmetic Industries, *Mar. Drugs*, 2018, **16**, 1–31.
84 R. Goralczyk, ß-Carotene and Lung Cancer in Smokers: Review of Hypotheses and Status of Research, *Nutr. Cancer*, 2009, **61**, 767–774.
85 R. M. Russell, Beta-carotene and lung cancer, *Pure Appl. Chem.*, 2002, **74**, 1461–1467.
86 A. Antunes, F. Carmo, S. Pinto, N. Andrade and F. Martel, The anti-proliferative effect of β-carotene against a triple-negative breast cancer cell line is cancer cell-specific and JNK-dependent, *PharmaNutrition*, 2022, **22**, 100320.
87 N. F. Gloria, *et al.*, Lycopene and Beta-carotene Induce Cell-Cycle Arrest and Apoptosis in Human Breast Cancer Cell Lines, *Anticancer Res.*, 2014, **34**, 1377–1386.
88 X. Hu, K. M. White, N. E. Jacobsen, D. J. Mangelsdorf and L. M. Canfield, Inhibition of growth and cholesterol synthesis in breast cancer cells by oxidation products of β-carotene 1, *J. Nutr. Biochem.*, 1998, **9**, 567–574.
89 X. Qi, *et al.*, Antioxidants in brain tumors: current therapeutic significance and future prospects, *Mol. Cancer*, 2022, **21**, 204.
90 T. Bohn, *et al.*, β-Carotene in the human body: metabolic bioactivation pathways – from digestion to tissue distribution and excretion, *Proc. Nutr. Soc.*, 2019, **78**, 68–87.
91 X.-C. Xu, Tumor-suppressive activity of retinoic acid receptor-β in cancer, *Cancer Lett.*, 2007, **253**, 14–24.
92 R. M. Connolly, N. K. Nguyen and S. Sukumar, Molecular Pathways: Current Role and Future Directions of the Retinoic Acid Pathway in Cancer Prevention and Treatment, *Clin. Cancer Res.*, 2013, **19**, 1651–1659.
93 R. Lotan, Lung Cancer Promotion by β-Carotene and Tobacco Smoke: Relationship to Suppression of Retinoic Acid Receptor-β and Increased Activator Protein-1?, *JNCI, J. Natl. Cancer Inst.*, 1999, **91**, 7–9.
94 P. Middha, S. J. Weinstein, S. Männistö, D. Albanes and A. M. Mondul, β-Carotene Supplementation and Lung Cancer Incidence in the Alpha-Tocopherol, Beta-Carotene Cancer Prevention Study: The Role of Tar and Nicotine, *Nicotine Tob. Res*, 2019, **21**, 1045–1050.
95 M. E. Wright, *et al.*, Effects of β-Carotene Supplementation on Molecular Markers of Lung Carcinogenesis in Male Smokers, *Cancer Prev. Res. (Phila. Pa.)*, 2010, **3**, 745–752.
96 Y.-J. Jeon, *et al.*, Effects of Beta-Carotene Supplements on Cancer Prevention: Meta-Analysis of Randomized Controlled Trials, *Nutr. Cancer*, 2011, **63**, 1196–1207.
97 J. Kordiak, F. Bielec, S. Jabłoński and D. Pastuszak-Lewandoska, Role of Beta-Carotene in Lung Cancer Primary Chemoprevention: A Systematic Review with Meta-Analysis and Meta-Regression, *Nutrients*, 2022, **14**, 1361.
98 A. Ruano-Ravina, A. Figueiras, M. Freire-Garabal and J. M. Barros-Dios, Antioxidant Vitamins and Risk of Lung Cancer, *Curr. Pharm. Des.*, 2006, **12**, 599–613.
99 N. Yu, X. Su, Z. Wang, B. Dai and J. Kang, Association of Dietary Vitamin A and β-Carotene Intake with the Risk of Lung Cancer: A Meta-Analysis of 19 Publications, *Nutrients*, 2015, **7**, 9309–9324.
100 M. Shareck, M.-C. Rousseau, A. Koushik, J. Siemiatycki and M.-E. Parent, Inverse Association between Dietary Intake of Selected Carotenoids and Vitamin C and Risk of Lung Cancer, *Front. Oncol.*, 2017, **7**, 1–12.
101 G. Sowmya Shree, *et al.*, β-carotene at physiologically attainable concentration induces apoptosis and down-regulates cell survival and antioxidant markers in human breast cancer (MCF-7) cells, *Mol. Cell. Biochem.*, 2017, **436**, 1–12.
102 G. Nagel, *et al.*, Dietary β-carotene, vitamin C and E intake and breast cancer risk in the European Prospective Investigation into Cancer and Nutrition (EPIC), *Breast Cancer Res. Treat.*, 2010, **119**, 753–765.
103 Y.-S. Kim, *et al.*, β-Carotene inhibits neuroblastoma cell invasion and metastasis *in vitro* and *in vivo* by decreasing level of hypoxia-inducible factor-1α, *J. Nutr. Biochem.*, 2014, **25**, 655–664.
104 C. N. Holick, E. L. Giovannucci, B. Rosner, M. J. Stampfer and D. S. Michaud, Prospective study of intake of fruit, vegetables, and carotenoids and the risk of adult glioma2, *Am. J. Clin. Nutr.*, 2007, **85**, 877–886.
105 J. Lin, *et al.*, Vitamins C and E and Beta Carotene Supplementation and Cancer Risk: A Randomized Controlled Trial, *JNCI, J. Natl. Cancer Inst.*, 2009, **101**, 14–23.
106 S. Hira, *et al.*, β-Carotene: A Natural Compound Improves Cognitive Impairment and Oxidative Stress in a Mouse Model of Streptozotocin-Induced Alzheimer's Disease, *Biomolecules*, 2019, **9**, 441.

 This journal is © the Owner Societies 2025